

# Modelling and crash simulation of long-fibre-reinforced thermoplastics

Thomas Seelig<sup>1</sup>, Arnulf Latz<sup>2</sup>, Sven Sanwald<sup>3</sup>

<sup>1</sup>Fraunhofer IWM, Wöhlerstr. 11, D-79108 Freiburg

<sup>2</sup>Fraunhofer ITWM, Fraunhofer-Platz 1, D-67663 Kaiserslautern

<sup>3</sup>Fraunhofer ICT, Joseph-von-Fraunhofer-Str.7, D-76327 Pfinztal

## Summary:

The presentation deals with the development, calibration and verification of a constitutive model for the deformation and failure of long-fibre-reinforced thermoplastics (LFT). The model has been implemented as a user-defined material model into LS-DYNA and is employed for the simulation of a component subjected to crash-loading. Numerical results are compared with respective experiments. Furthermore, a methodology to incorporate in crash simulations the spatial distribution of fibre orientation in the component determined from preceding simulations of the manufacturing process is discussed.

## Keywords:

Fibre-reinforced thermoplastics, constitutive modelling, process chain, fibre orientation distribution, crash simulation

## 1 Introduction

Thermoplastic polymers such as polypropylene (PP) or polyamide (PA) reinforced by glass fibres more than 10mm long – so-called long-fibre-reinforced thermoplastics (LFT) – have gained increasing attention in recent years. Their superior mechanical properties compared to “classical” short-fibre-reinforced thermoplastics (fibre length < 1mm) in conjunction with improved manufacturing techniques (e.g. pressure moulding) which minimize the fibre length reduction (breaking) during processing render them an attractive material for structural (e.g. automotive) applications. This, however, requires a reliable predictability of the mechanical performance of respective components by numerical simulations for which appropriate models for the material behaviour of LFT are needed. Constitutive modelling of LFT materials and whole components is complicated by the fact that the long fibres lead to a strong anisotropy of the material and that due to the melt flow during processing the strength and direction (fibre orientation) of this anisotropy vary significantly throughout a final component (Fig. 1).

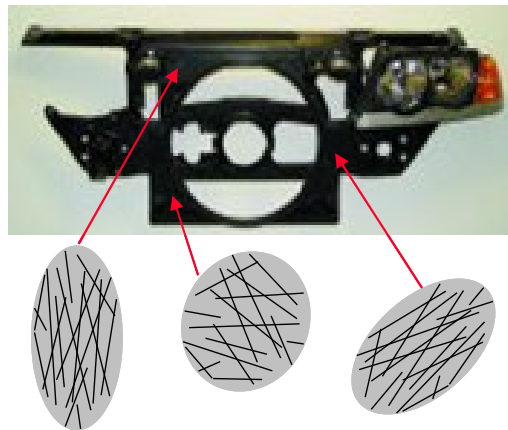


Fig. 1: Typical automotive component made from LFT and schematic of spatially varying fibre orientation

Despite knowledge of these issues, simulations in practice are mostly based on isotropic and/or linear elastic material models which induce a large amount of uncertainty in the predicted component behaviour. Aiming at an improvement of the accuracy of numerical simulations of components made from LFT materials, the purpose of the present work is to develop

- appropriate models for the constitutive description of LFT and
- a methodology to take the spatially varying material anisotropy in a component into account.

The latter is accomplished by modelling of the whole process chain, i.e. by computing the fibre orientation distribution from mould filling simulations and mapping this information onto the computational model for structural analyses.

## 2 Experimental characterization of LFT material

In order to determine the mechanical behaviour in tension and compression tests, specimens were cut from compression moulded plates of the LFT material PP-GF30 with 12mm fibre length. Due to the melt flow during processing a pronounced fibre orientation prevails in these plates. In the following the principal direction of the fibre orientation (i.e. the flow direction) and the transverse direction are referred to as 0° and 90° directions, respectively.

Figure 2 shows experimental results (thin coloured curves) from quasistatic tests under uniaxial tension (left) and compression (right) for both directions. For tension as well as compression the material behaviour displays a strong anisotropy with a pronounced nonlinearity in the 90° (transverse) direction owing to the dominance of the ductile matrix. In the 90° direction a significantly higher stress is observed under compression than under tension. This tension-compression asymmetry results from a higher compressive yield stress of the polymer matrix as well as from a stronger stiffening effect of the embedded fibres under transverse compression. Under tensile loading (Fig. 2a) the material

undergoes brittle failure at about 2% strain in the 0° direction and about 4% in the 90° direction. Under compression (Fig. 2b) inhomogeneous specimen deformation (e.g. buckling or kinking) sets in at approximately the same level of strain, hence experimental results are shown only for the range of meaningful stress/strain evaluation. Also depicted in Fig. 2 is the response of the constitutive model discussed in Sect. 3.

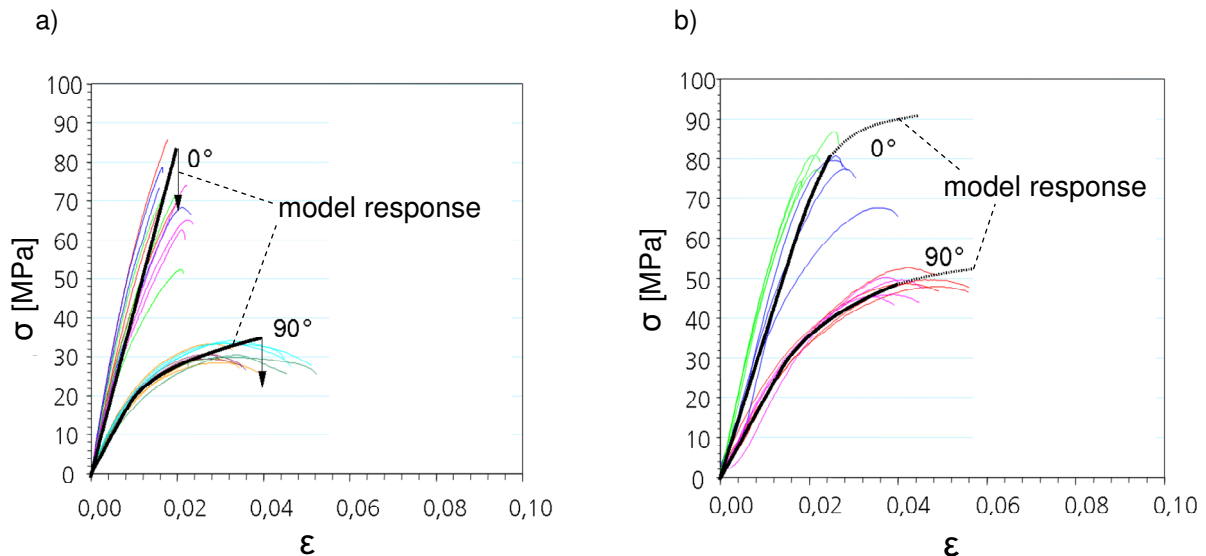


Fig. 2: Experimental data and model response in terms of engineering stress vs. engineering strain under uniaxial tension (a) and compression (b) along principal fibre direction (0°) and in transverse direction (90°)

The failure mechanisms leading to the different fracture strains of 2% and 4%, respectively, under tensile loading can be analyzed from the micrographs of the fracture surfaces shown in Fig. 3. Tension in the principal fibre direction (0°, Fig. 3a) gives rise to fibre rupture or pull-out with only a small amount of matrix deformation whereas tension in the transverse direction (90°, Fig. 3b) leads to fibre-matrix debonding accompanied by massive plastic matrix deformation.

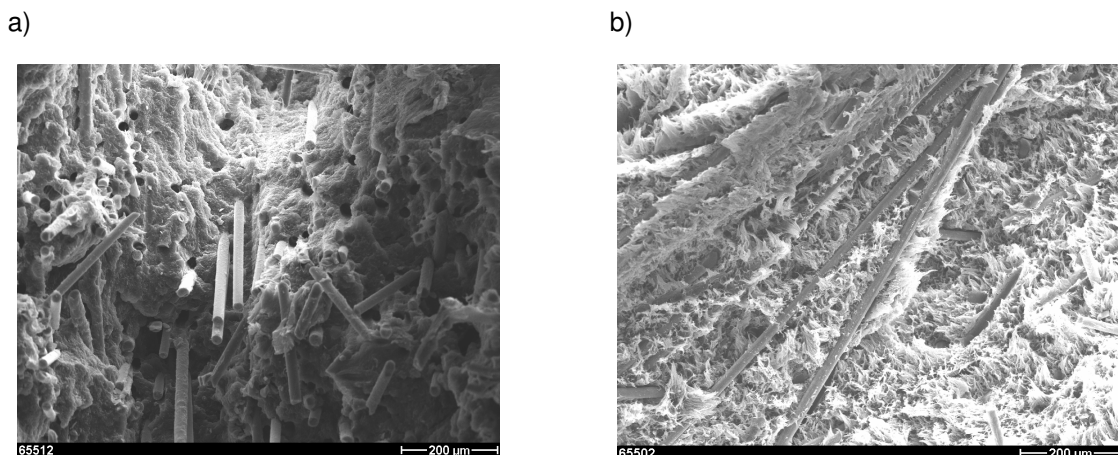


Fig. 3: Micrographs of fracture surfaces after tension tests in 0° direction (a) and 90° direction (b)

### 3 Constitutive modelling

The strongly anisotropic elastic-plastic behaviour of LFT materials in conjunction with the pronounced tension-compression asymmetry cannot be described by constitutive models currently available in LS-DYNA. Therefore, the following model has been developed and implemented as a user-subroutine for solid as well as shell elements.

### 3.1 Deformation behaviour

The model is based on the approximation of the material behaviour as elastically and plastically transversely isotropic with the principal fibre direction taken as the 1-direction of a local (material) coordinate system and the 2- and 3-directions lying in the plane of isotropy. The elastic behaviour is determined by five material constants (see, e.g., [4]) while plastic yielding is governed by the yield condition

$$\sigma_e + \alpha \sigma_m \leq \sigma_F(\varepsilon_p) \quad (1)$$

where the purely deviatoric equivalent stress [1]

$$\sigma_e = \left\{ b \left[ \sigma_{11} (\sigma_{11} - \sigma_{22} - \sigma_{33}) + \sigma_{22} \sigma_{33} - \sigma_{23}^2 \right] + (\sigma_{22} - \sigma_{33})^2 + 4\sigma_{23}^2 + a \left[ \sigma_{12}^2 + \sigma_{13}^2 \right] \right\}^{1/2} \quad (2)$$

contains two parameters  $a$  and  $b$ , and  $\sigma_m = (\sigma_{11} + \sigma_{22} + \sigma_{33})/3$  is the hydrostatic stress introduced in (1) to describe the tension-compression asymmetry discussed above via a constant pre-factor  $\alpha > 0$ . The yield stress

$$\sigma_F(\varepsilon_p) = \sigma_0 + h\varepsilon_p^n \quad (3)$$

is for simplicity represented by an isotropic hardening law with constants  $\sigma_0, h, n$  and the equivalent plastic strain  $\varepsilon_p$ . Isochoric plastic flow is described by the non-associate flow rule

$$D_{ij}^p = \lambda \frac{\partial \sigma_e}{\partial \sigma_{ij}} \quad (4)$$

for the plastic strain rate  $D_{ij}^p$  where the pre-factor  $\lambda$  is in case of a rate-independent model computed from the equality in (1). The model can be extended to a rate-dependent one by replacing  $\lambda$  by an additional constitutive relation for the equivalent plastic strain rate. Its calibration then requires additional experimental data at different strain rates.

### 3.2 Failure criterion

The above model for the deformation behaviour of LFT materials is supplemented with a failure criterion which is active only under tensile loading and predicts failure at critical strains of

$$\varepsilon_{11}^{crit} = 0.02 \quad \text{or} \quad \varepsilon_{22}^{crit} (= \varepsilon_{33}^{crit}) = 0.04 \quad (5)$$

corresponding to the experimental findings (see Fig. 2a). Local failure is modelled by elimination of finite elements once this criterion is met (at a user-specified number of thickness integration points in case of shell elements).

### 3.3 Model verification

The response of the model is shown in Fig. 2 (thick black curves) in comparison with the experimental results used for calibration of the model. Under compressive loading (Fig. 2b) experimental stress-strain data are available only for the range of homogeneous specimen deformation, the behaviour of the material model is extrapolated beyond that range according to the dotted black curves in Fig. 2b.

Without any further adjustment of material parameters the model described in Sects. 3.1 and 3.2 has been employed to simulate three-point-bending tests as shown in Fig. 4a. The slender specimens were cut in  $0^\circ$  direction and  $90^\circ$  direction from the same plates of the LFT material as the tension and compression specimens before. Results of various experiments as well as the numerical simulations are depicted in Figs. 4b and c. Except for the somewhat too early failure predicted by the simulation of

the 0° test the results are in good agreement and suggest the applicability of the model (calibrated from tension and compression tests only) to more complex situations.

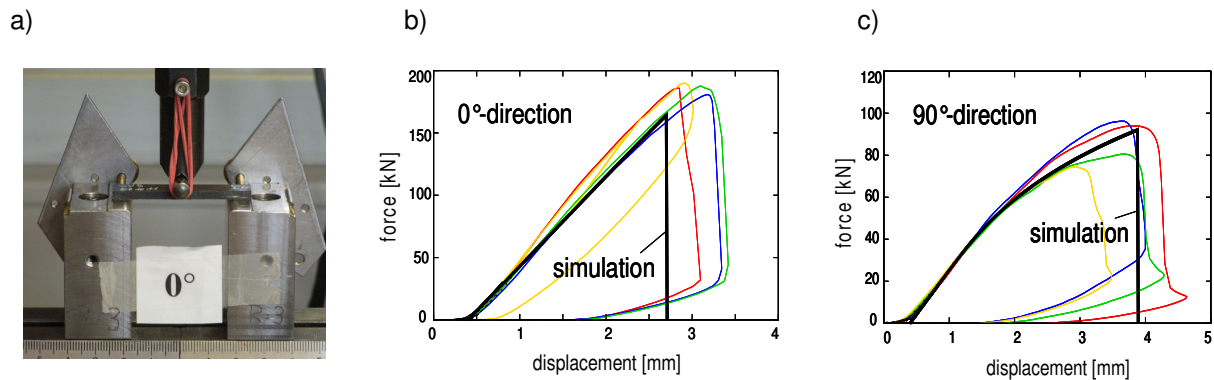


Fig. 4: a) Experimental set-up of three-point-bending tests, b) and c) experimental and numerical results for two different specimen orientations with respect to principal fibre direction

#### 4 Fibre orientation distribution

In complex-shaped real components manufactured from LFT materials the strength and direction (i.e. principal axes) of the fibre orientation typically display strong spatial variations. It can hence be expected that the mechanical behaviour of such a component depends on the spatial variation of the corresponding material anisotropy. The latter can be accounted for by different methodologies. One may, for instance, cut specimens for the determination of local material properties from a prototype component at various locations, which is cumbersome and expensive – especially since the prototype has to be produced first. Another, much cheaper, way consists of a material characterization from pre-manufactured plates/specimens (as in Sect. 2) and *assuming* the directions of local material anisotropy in the component. Simulations for different variants of such an assumed fibre orientation distribution in the component then may (at least in the range of monotonic loading) lead to upper and lower bounds of its real behaviour.

An alternative approach, suggested and employed in the present work, is based on the virtual modelling of the whole *process chain*, i.e. the numerical simulation of the mould filling process to predict the fibre orientation distribution in the component and the utilization of this information in the subsequent structural analysis (e.g. crash simulation). Existing commercial codes for the simulation of mould filling processes, however, are based on models (e.g. short fibres in dilute suspension) not sufficient for the situation of LFT materials. More advanced and appropriate models for the fibre-fluid interaction have been developed in recent years [3] and are employed in the present work.

Figure 5a shows the pressure moulded component investigated in the present work in order to check the developed models and the methodology of combining mould filling and crash simulations via mapping of the predicted fibre orientation distribution. The component consists of the same LFT material (PP-GF30 with 12mm fibre length) as considered in Sect. 3. It has a wall thickness of about 3mm and contains in one direction a thicker part (stiffening rib) of 11mm thickness) along its middle axis as sketched in Fig. 5b.

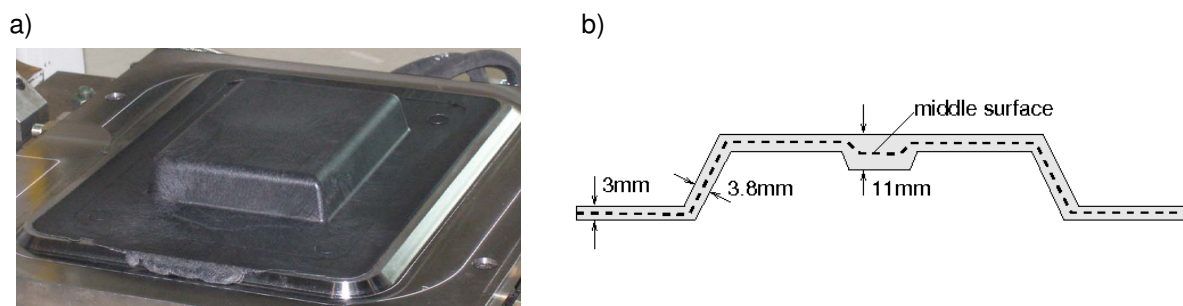


Fig. 5: Compression moulded component (a) and cross section showing wall thickness (b)

In terms of one component of the second order fibre orientation tensor [2]

$$\mathbf{a} = \sum_{i=1}^3 a_i \vec{e}_i \otimes \vec{e}_i. \quad (6)$$

computed from the mould filling simulation, the spatial fibre orientation distribution in the component is depicted in Fig. 6a. In the (spectral) representation (6)  $\vec{e}_i$  and  $a_i$  denote eigenvectors and eigenvalues, respectively, where  $a_1 + a_2 + a_3 = 1$  and  $a_i = 1/3$  corresponds to an isotropic fibre orientation. The orientation distribution is mapped onto the finite element model shown in Fig. 6b which consists of about 4600 four-node shell elements along the component middle surface indicated in Fig. 5b. In each finite element integration point the 1-axis of the local coordinate system for the constitutive model of Sect. 3 is determined by the local principal axis  $\vec{e}_1$  of the computed fibre orientation tensor (6).

Whereas detailed information about the fibre orientation distribution in the component is available from the mould filling simulation, the solid mechanical behaviour of the material (i.e. the material parameters of the constitutive model according to Sect. 3) is known only for the single state of pronounced fibre orientation prevailing in the tested specimens. To establish a correlation between the computed fibre orientation and the calibrated anisotropic material behaviour, the latter is assigned only to those points with a computed maximum eigenvalue of the fibre orientation  $a_1 > 0.7$ . In points of the component with  $1/3 < a_1 < 0.7$  an isotropic material behaviour with properties averaged from the measured 0°- and 90°-responses (see Sect. 3.1) is assumed.

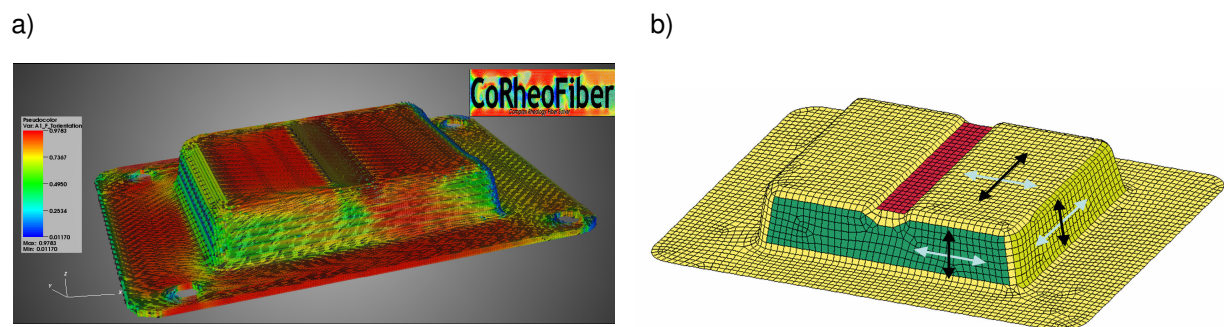


Fig. 6: Fibre orientation distribution from mould filling simulation (a) and finite element model of the component (b)

For comparison of numerical results (see Sect. 5, Fig. 8) also the approach with different variants of an assumed fibre orientation (not using information from mould filling simulation) is considered in the structural analyses. These assumed fibre orientations in the different parts of the component are indicated by the arrows in Fig. 6b.

## 5 Component test and simulation

The experimental set-up of the crash test with the LFT component clamped along its boundary in a steel frame is shown in Fig. 7. Quasistatic loading was imposed via a spherical indenter at the centre of the component. The measured force as a function of indenter displacement is depicted in Fig. 8 (red curve) along with results from different numerical simulations (discussed below). After a linear rise an abrupt load drop occurs as the thick stiffening rib breaks (visible in Fig. 9b). Subsequently several cracks form and spread in different directions throughout the component with increasing displacement of the indenter.

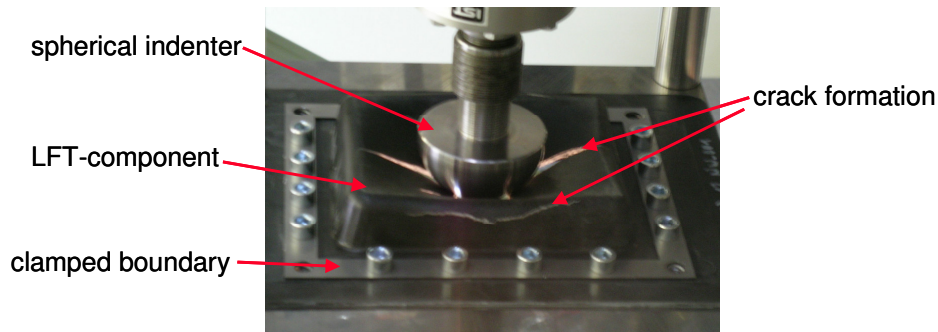


Fig. 7: Experimental set-up of component test

Numerical results are shown in Fig. 8 for the simulation with the fibre orientation (i.e. anisotropy) distribution determined and mapped from the numerical mould filling analysis (green curves) and for simulations based on two assumed (fictitious) fibre orientations according to the arrows in Fig. 6b. (black and blue curves). Obviously, a much better agreement between the real (experimental) component behaviour and the numerical simulation can be achieved when the information with respect to the fibre orientation distribution from the mould filling simulation is utilized. The initial slope of the load-displacement curve, the peak load, the instant of first dramatic failure as well as the subsequent response are well captured – in contrast to the simulations based only on crude assumptions of the fibre orientation (black and blue curves in Fig. 8).

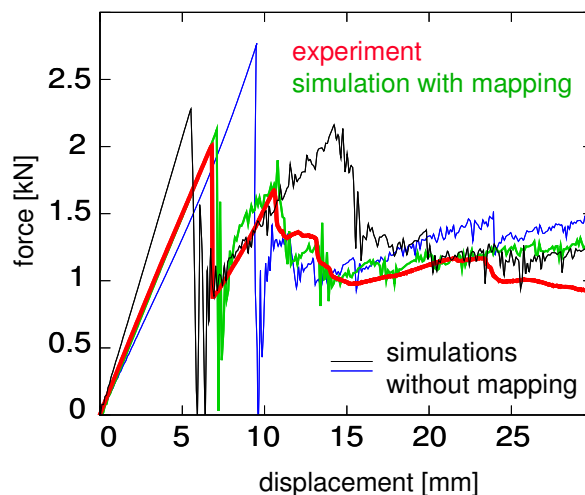


Fig. 8: Experimental and simulated load displacement curves

A comparison of the crack pattern in the component resulting from the component test with that obtained from the numerical simulation (using the mapped fibre orientation distribution) is shown in Fig. 9. It illustrates that besides the overall behaviour also details of the failure process are well predicted by the model.

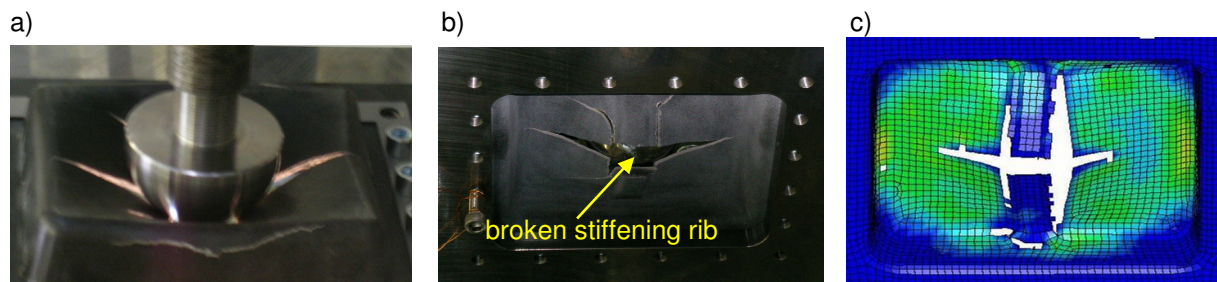


Fig. 9: Crack pattern in component (a: top view, b: bottom view) and finite element model (c)

## 6 Summary

We have presented an experimental characterization (tension and compression tests in two orthogonal directions) of a typical LFT material (PP-GF30) and have developed a rather simple transversely isotropic elastic-plastic constitutive model that captures the key features of the observed material behaviour, i.e. strong anisotropy with a pronounced nonlinearity in matrix dominated directions and tension-compression asymmetry. Moreover, a methodology has been developed to incorporate in structural finite element analyses of a whole LFT component information with regard to the local strength and direction of the material anisotropy obtained (in terms of the fibre orientation distribution) from simulations of the manufacturing (mould filling) process.

One weak point in this virtual process chain is the correlation between the local state of fibre orientation and the material parameters of the constitutive model which have to be determined from experiments and are available only for those fibre orientation states prevailing in the tested specimens. Micromechanical models and virtual testing of representative volume elements of the microstructure of LFT materials with different fibre orientation states may help to gain additional information while keeping the number of real experiments limited and affordable.

Though in the present work the correlation between computed fibre orientation distribution and solid mechanical material behaviour has been established in a rather crude manner, it helped to significantly improve the prediction of the crash simulation of a real LFT component. The constitutive model for LFT materials presented here may (and needs to) be extended in various regards, the most important aspect being the rate-dependence which is significant for polymeric materials and may have a strong influence on the behaviour of LFT components subjected to high-rate loading.

## 7 Literature

- [1] Aravas, N.: Finite elastoplastic transformations of transversely isotropic metals. Int. J. of Solids and Structures 29, 1992, 2137-2157.
- [2] Folgar, F., Tucker, C.L.: Orientation behavior of fibers in concentrated suspensions. J. of Reinforced Plastics and Composites 3, 1984, 98-119.
- [3] Strautins, U., Latz, A.: Flow driven orientation dynamics of flexible long fiber systems. Rheologica Acta 46, 2007, 1057-1064.
- [4] Ward, I.M., Hadley, D.W.: An Introduction to the Mechanical Properties of Solid Polymers. John Wiley & Sons, 1993.